ISSN 1064-2269, Journal of Communications Technology and Electronics, 2007, Vol. 52, No. 8, pp. 932–937. © Pleiades Publishing, Inc., 2007.
Original Russian Text © V.A. Komotskii, S.M. Okoth, Yu.M. Sokolov, 2007, published in Radiotekhnika i Elektronika, 2007, Vol. 52, No. 8, pp. 1006–1012.

PHYSICAL PROCESSES IN ELECTRON DEVICES

Technique and Results of Measuring Surface-Acoustic-Wave Reflection Coefficients with the Use of Laser Sounding

V. A. Komotskii, S. M. Okoth, and Yu. M. Sokolov

Received December 1, 2005

Abstract—A technique of measuring the surface-acoustic-wave (SAW) reflection with the use of a laser sounding facility containing a reference diffraction grating is described. The characteristics of the SAW reflections from the edges of *YX*-cut quartz-crystal substrates with the end faces beveled at various angles are measured. In addition, the frequency dependence of the magnitude of the SAW reflection coefficient for reflection from periodic gratings in the form of lithium niobate metal strips are measured.

PACS numbers: 42.62.-b, 77.65.Dq

DOI: 10.1134/S1064226907080141

INTRODUCTION

Surface-acoustic-wave (SAW) reflecting elements are widely used in acoustoelectronic devices. The development of experimental methods for measuring SAW reflection characteristics may be of interest to both the specialists designing acoustoelectronic devices and the researchers studying physical phenomena occurring when SAWs are reflected from various objects. In this paper, a technique for investigating the SAW reflection characteristics on the basis of SAW laser sounding with the use of a reference diffraction grating (RDG) [1] is employed and developed further. This procedure allows detailed direct measurements of the magnitude of the reflection coefficient as a function of the SAW frequency [2] and thus significantly extends the possibilities of the widely known methods for measuring SAW reflection: the pulse method [3–5] and the interference method [6].

1. MEASUREMENT SCHEME AND TECHNIQUE

The scheme of the SAW laser sounding with the use of an RDG (Fig. 1) was earlier described in [7–9]. The sounding laser beam passes through the reference phase diffraction grating and is directed toward the substrate over which the SAW propagates. The beam reflects from the substrate, undergoes phase spatial modulation owing to the presence of the SAW, and then passes through the RDG for the second time. RDG period Λ_g is chosen equal to SAW wavelength Λ; however, the relation $\Lambda = \Lambda_g$ remains valid only at single SAW frequency F_0, which is usually the midband frequency of the measurement frequency range. As SAW frequency F deviates from F_0, the signal amplitude decreases owing to the mismatch between the periods of the grating and the SAW within the limits of aperture D of the optical beam. Frequency bandwidth ΔF within which the measurements can be conducted without replacement of the RDG depends on ratio $D/\Lambda = N_g$, i.e., on the number of the grating grooves falling within the aperture of the sounding laser beam. Bandwidth ΔF can be estimated from the relationship [8] $\Delta F \approx F_0/2N_g$.

The sounded area of the substrate is coated with a thin reflecting metal film, which improves the lasing efficiency and prevents the interferences that can occur when the laser radiation is scattered by the waves propagating inside the substrate, under its surface. From the diffraction pattern resulting from the interaction with the RDG–SAW system, the zeroth diffraction order is usually separated. The radiation power in the zeroth diffraction order oscillates with the SAW frequency. In this case, if a traveling wave propagates in the substrate, the amplitude of oscillations of light power $P_0^{(F)}$ contained in the zeroth diffraction order is proportional to the amplitude of the corrugation of the traveling SAW propagating over the substrate; i.e.,

$$P_0^{(F)} = q_0^{(F)} a_s P_{\text{eff}} = q_0^{(F)} a_s P_1 k_{\text{loss}},$$

where $q_0^{(F)}$ is the efficiency factor, which depends on the RDG properties and the parameters of the optical scheme [7–9]; a_s is the amplitude of the surface corrugation produced by the SAW; P_1 is the lasing power; k_{loss} is the loss coefficient describing losses of the radiation power in the optical system that are due to the reflection and absorption of light; and $P_{\text{eff}} = P_1 k_{\text{loss}}$ is the effective power of the sounding radiation, which can be considered equal to the total power of all diffraction orders at the output of the optical system.

During experiments, we usually use a phase diffraction grating with a rectangular meander-shaped profile.

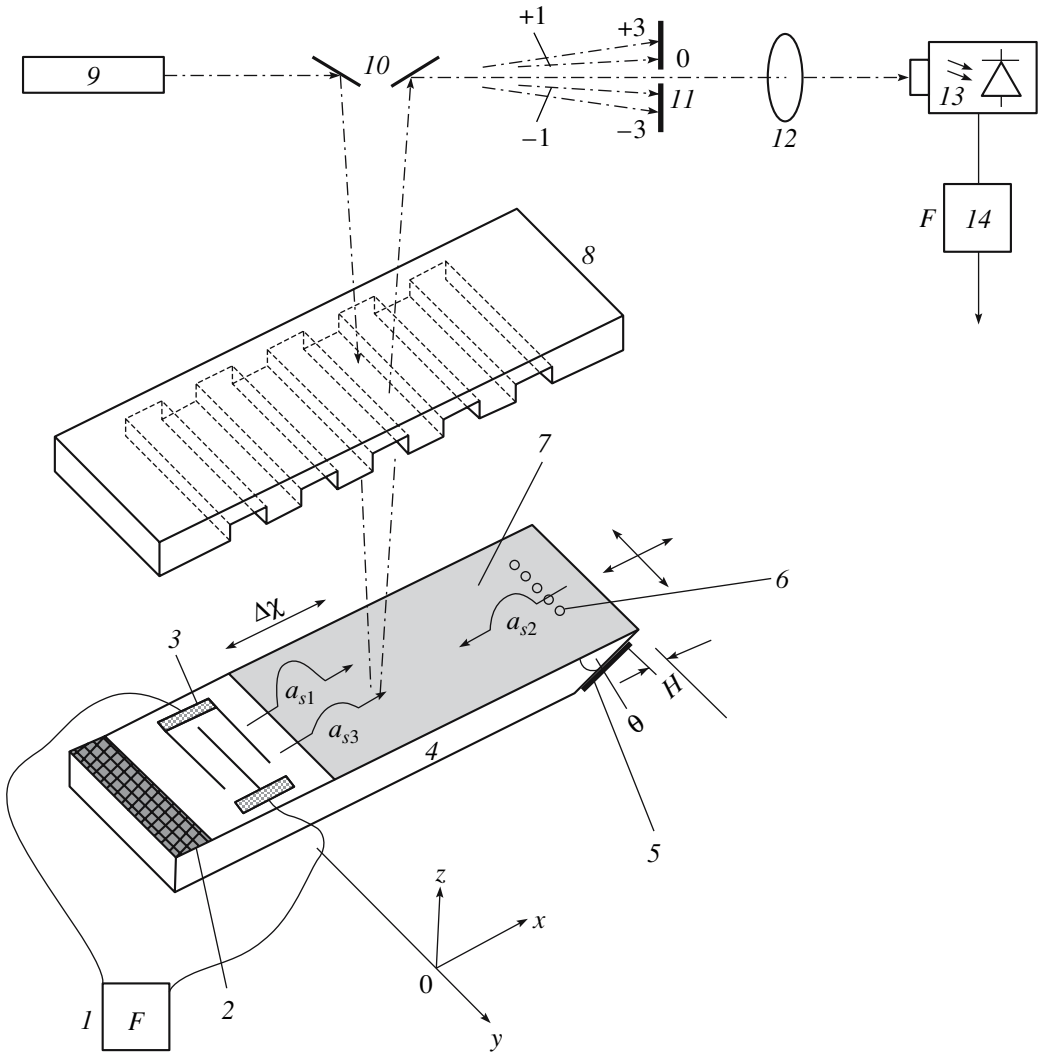

Fig. 1. Layout of the SAW reflection sounding setup with the RDG detached: (*1*) generator, (*2*) SAW absorber, (*3*) SAW launcher (IDT), (*4*) substrate, (*5*) SAW absorber on the end face, (*6*) sounding spots, (*7*) reflecting metal film, (*8*) RDG, (*9*) laser, (*10*) mirrors, (*11*) spatial filter, (*12*) lens, (*13*) photodetector with a load, and (*14*) amplifier in the laser-sounding channel

The optimum RDG depth corresponds to the amplitude of the spatial phase modulation of the optical wave front, $\Phi_M = 22.5°$. If the grating is made as a relief on glass with the refractive index $n_{gl} = 1.51$, the height of the relief is $h = \lambda\Phi_M/\pi(n_{gl} - 1)$.

At the lasing wavelength $\lambda = 0.6328$ μm, we obtain $h = 155$ nm. In the case of detection of the signal in the zeroth order and the optimum height of the RDG located close to the substrate, the efficiency factor is $q_0^{(F)} = 0.63$, which corresponds to the maximum efficiency of conversion of the SAW signal into the power oscillations in the diffraction order. In addition, the signal at the SAW frequency can be obtained if the photodetector is placed in one of the first diffraction orders; however, in this case, the signal level will be half the signal level obtained with the photodetector placed in the zeroth order [7–9].

The photodetector converts the zeroth-order power oscillations into an electric signal with a frequency equal to the SAW frequency. This signal can be written as

$$U(t) = U_m^{(F)}\cos(2\pi Ft + \varphi).$$

Signal amplitude $U_m^{(F)}$ is proportional to SAW amplitude a_s. Signal phase φ is linearly dependent on the SAW phase in the sounding area. If the substrate with the traveling wave is shifted in the direction of the SAW propagation (along the $0x$ axis) by Δx, the phase of the power oscillations in the diffraction orders changes by $\Delta\varphi = (2\pi/\Lambda)\Delta x$.

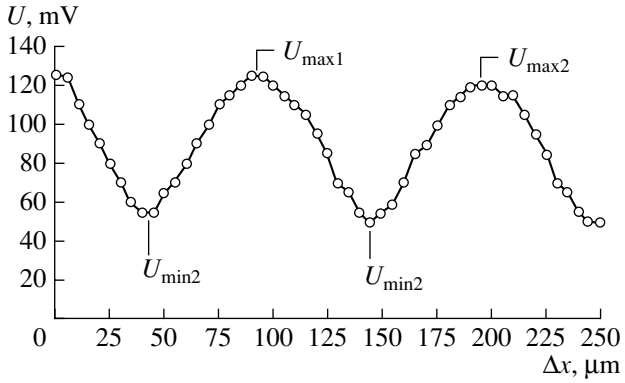

Fig. 2. Experimental dependence of amplitude U of the output signal on longitudinal shift Δx of the substrate. The shift step is 5 μm.

If two surface waves (a forward wave with amplitude a_{s1} and a reflected wave with amplitude a_{s2}) travel over the substrate in opposite directions, the signal with SAW frequency F at the photodetector output is a superposition of two partial signals, responses to these waves, with oscillation amplitudes $U_{m1}^{(F)}$ and $U_{m2}^{(F)}$. When the substrate is shifted in the $0x$ direction, the phase shifts of these partial signals are opposite in sign: $\Delta\varphi_1 = (2\pi/\Lambda)\Delta x$ and $\Delta\varphi_2 = -(2\pi/\Lambda)\Delta x$. As a result, if the substrate is shifted along the $0x$ axis, the amplitude of the sum signal at frequency F varies with a period equal to the SAW half-wave, $\Lambda/2$. In this case, the maximum signal amplitude corresponds to in-phase summation of the oscillations with frequency F and is expressed as $U_{\max} = U_{m1}^{(F)} + U_{m2}^{(F)}$. The minimum amplitude is $U_{\min} = U_{m1}^{(F)} - U_{m2}^{(F)}$. The ratio $K_{\rm st} = U_{\max}/U_{\min}$ is, in effect, the same as the SAW standing-wave ratio (SWR) because

$$K_{\rm st} = \frac{U_{\max}}{U_{\min}} = \frac{U_{m1}^{(F)} + U_{m2}^{(F)}}{U_{m1}^{(F)} - U_{m2}^{(F)}}$$

$$= \frac{a_{s1} + a_{s2}}{a_{s1} - a_{s2}} = \frac{a_{\max}}{a_{\min}} = \text{SWR}.$$

Thus, having measured $U_{\max}$ and $U_{\min}$ with the substrate shifted along the $0x$ axis through distance $\Delta x > 0.5\Lambda$, we can calculate $K_{\rm st}$ and then find the SAW reflection coefficient by using the known formula $|R| = (K_{\rm st} - 1)/(K_{\rm st} + 1)$.

By varying the SAW frequency and repeating the measurements, we can obtain the magnitude of the reflection coefficient as a function of frequency with a required frequency resolution. Similar measurements can be performed if the substrate is fixed and the RDG is shifted along the $0x$ axis. In this case, in addition, the phase shifts of the partial oscillations are opposite in sign and the period of variation in the output signal caused by the RDG displacement is $0.5\Lambda_{\rm g}$.

A typical experimental plot of the amplitude of the output signal as a function of the substrate shift, function $U_m(x)$, is shown in Fig. 2. This dependence is obtained via sounding of an SAW with the frequency $F = 17.4$ MHz that propagates over a *YZ*-cut lithium niobate substrate. The period of the obtained plot is approximately 100 μm, which corresponds to the SAW half-wavelength ($\Lambda \approx 200$ μm).

During tuning of the experimental facility, measures should be taken to prevent direct pickup of an interfering signal with the SAW frequency at the amplification stage of the optical sounding channel. This interference causes an additional periodic dependence of the amplitude of the output signal on the substrate shift with period Λ rather than $\Lambda/2$. This effect may distort the measurement results. During the experiment, the direct-pickup interference was monitored with an S4-25 spectrum analyzer and its value was lower than –55 dB with respect to the level of the desired signal. The interference level was measured with the sounding beam stopped by a screen.

2. MEASUREMENT RESULTS

The magnitude of the reflection coefficient was measured for the following objects:

(1) edges of the crystalline-quartz substrates with end faces beveled at various angles and

(2) periodic structures on the surface of a lithium niobate substrate formed out of strips of thin metal film, the strip periods being equal to the SAW wavelength (Λ) and half-wavelength (0.5Λ).

Reflections from substrate ends. Fourteen 2-mm-thick substrate samples were manufactured from *YX*-cut crystalline quartz. The end faces of the substrates were beveled at various angles to the surface (55°, 60°, 62°, 65°, 67°, 70°, 73°, 75°, 77°, 80°, 82°, 85°, 87°, and 90°). The surfaces and the end faces of the substrates were polished to obtain a grade-14 surface finish. Each substrate surface contained an interdigital transducer (IDT) with 12 pairs of fingers, which was placed on the substrate surface. The use of a relatively small number of pairs was due to the desire to reduce the effect of secondary reflections of the backward wave on the measurement data, i.e., to reduce the effect of the so-called three-pass signal. Each sample was used to measure the magnitude of the reflection coefficient, $|R|$, at various frequencies (50 frequencies with a step of 20 kHz in the frequency range 15.5–16.5 MHz). Some of the obtained curves of $|R(F)|$ are given in Fig. 3. The behavior of these curves indicates that the magnitude of the reflection coefficient is practically frequency independent. Small oscillatory deviations with

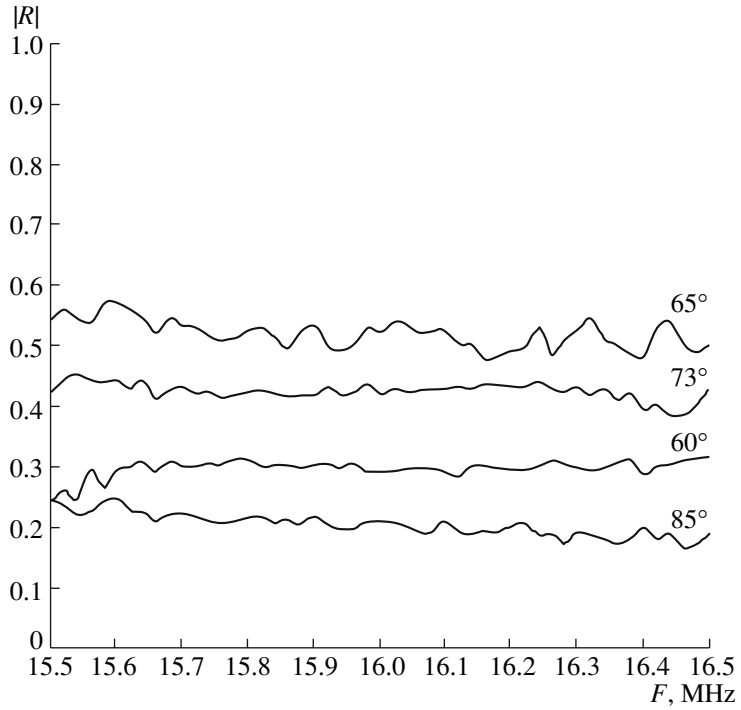

Fig. 3. Magnitude of the SAW reflection coefficient as a function of frequency for four bevel angles of the substrate's end face.

a period of the order of 70–80 kHz could be caused by either reflections of the indirect wave from the IDT or generation of stray SAWs due to the reflections and scattering of the bulk waves radiated by the IDT.

It should be noted that, in this experiment, we used SAW absorbers in order to reduce or eliminate the effect of all possible unwanted waves. One absorber was placed at the end of the substrate opposite to the beveled end, while the other absorber was placed on the beveled end face of the substrate so that the end face had an absorber-free area of depth H equal to ~2–3Λ and adjacent to the reflecting edge (see Fig. 1). In the absence of an absorber on the end face of the substrate, we observed distortions of the measurement data caused by the return of the wave that passed to the end-face plane and reflected from the lower edge of the end face. This effect showed itself as an added periodic variation in the frequency dependence of $|R|$ with a period of the order of 700 kHz. The effect was removed by placing an absorber on the end face of the substrate. In order to improve the reliability of the results, similar measurements of magnitude $|R(F)|$ of the reflection coefficient were conducted at five different points distributed over the aperture of the SAW radiator (see Fig. 1). Later, the measurement results were averaged over frequency and over the measurement positions. The mean values of both the magnitude of the reflection coefficient ($|R|_{\text{mean}}$) and the rms deviation (σ_R) are given in the table.

The analysis of this data shows a strong dependence of the magnitude of the reflection coefficient on bevel angle Θ of the end face. Minimum values of $|R|$ were observed at angles of 60°, 70°, 80°, and 84°; maximum values were observed at angles of 67° and 73°; and an increase in $|R|$ was observed near the end of the measurement range at angles of 85° through 90°. The variations roughly agree with the behavior of the curves

Magnitude $|R|_{\text{mean}}$ of the reflection coefficient and rms deviation σ_R at various bevel angles of the substrate's end face

θ, deg	$\lvert R\rvert_{\text{mean}}$	σ_R
55	0.29	0.021
60	0.29	0.016
62	0.37	0.019
65	0.52	0.023
67	0.66	0.016
70	0.33	0.022
73	0.43	0.009
75	0.30	0.010
77	0.25	0.017
80	0.16	0.029
82	0.21	0.022
85	0.21	0.015
87	0.41	0.008
90	0.46	0.018

given in [4–6]. The best possible comparison can be made with the data given in [6], since the experiments described in [6] were likewise conducted with substrates made of *YX*-cut crystalline quartz. At angles of 60° to 75°, the data are in good agreement. However, at angles of 80° to 85°, the values of the reflection coefficient obtained from our measurement data are much lower.

Reflections from periodic structures. The structures under investigation consisted of 80-nm-thick separate strips of thin copper film located on the surfaces of *YZ*-cut lithium niobate substrates. Measured with an error of 3%, the widths of the metal strips and of the gaps between the strips were the same. To perform the measurements, periodic structures of two types were manufactured. The first type of structure had the period $l_1 = 100$ μm, which corresponds to a half-wavelength of the wave excited by the IDT at its center frequency (the 0.5Λ type). The second type of structure had the period $l_2 = 200$ μm, which corresponds to a half-wavelength of the wave excited by the IDT at its center frequency (the Λ type). The IDT had five pairs of electrodes and an 8-mm aperture and was located at a distance of 18 mm from the reflecting structure on the samples of the first type and at a distance of 6 mm from the reflecting structure on the samples of the second type. Between the IDT and the reflecting structure, there was an area coated with a metal film measuring 3 mm in the longitudinal direction and 8 mm in the transverse direction. The number of strips in the gratings of both types was $N = 40$. The strips were isolated from each other. To measure the reflecting properties of the structures with a smaller number of strips, an SAW absorber was glued onto a part of the reflecting structure and the measurements were repeated.

The measurements were usually performed in the frequency range 1.0–1.5 MHz, the frequency step being 0.02 MHz. The signal from a G4-158 crystal-controlled generator was applied to the IDT. The signal was measured by a V6-10 selective voltmeter using a 9-kHz channel.

Typical plots of the magnitude of the reflection coefficient as a function of frequency are shown in Fig. 4. Curves *1* and *2* correspond to the measured magnitudes of the reflection coefficient for the first type of structure ($l_1 = 100$ μm). Curves *3* and *4* correspond to the magnitudes of the reflection coefficient for the second type of structure ($l_2 = 200$ μm).

It is very interesting that the reflection from a structure with the period $l_2 = 200$ μm is greater than the reflection from a structure with the period $l_1 = 100$ μm. The shapes of the frequency dependences of the reflection coefficient are sufficiently close to the plot of function $\sin u/u$. The width of the main lobe of this characteristic is 0.45 MHz at $N = 40$. Being related to the center frequency of the frequency characteristic $F_0 = 17.3$ MHz, this value is approximately $\Delta F/F_0 \approx 1/38$, i.e., of the order of $1/N$. It is significant that, as the number of the reflecting strips is reduced from 40 to 18, the reflection coefficient is reduced from 0.95 to 0.70 and the width of the main peak is virtually doubled.

The SAW reflection from the structures under consideration is mainly due to the change in the velocity of the SAW propagation, Δv, that occurs when the wave travels over the segments covered with the metal film ($|\Delta v/v| = 2.4 \times 10^{-3}$) [10]. This statement was confirmed convincingly by the following experiment with the second type of structure. A continuous copper film with a thickness of about 100 nm was sputtered onto the surface of the reflecting structure. The measurements performed according to the above-described procedure and with the use of the sample with an additional conducting coating have shown that the reflection coefficient from this short-circuited structure was lower than 5% at the center frequency and about 1–2% (within the limits of error) outside the maximum-reflection band of the Λ-type structure.

The reflecting properties of the 0.5Λ-type structure are described in [10, 11] and used widely in engineering. During physical interpretation of the Bragg reflection from a periodic structure formed by crests and troughs located at intervals of Λ/2, it was assumed [11] that the reflection coefficient from an upward-step boundary differs in phase by 180° from the reflection coefficient from a downward-step boundary. This circumstance results in an in-phase summation of the waves reflected from different boundaries. Strong reflections from the Λ-type structure, which were observed in our experiments, were not mentioned in [10, 11].

In the experiments, sufficiently high values of the reflection coefficient were obtained for both types of structures (0.5Λ and Λ). If, by analogy with [11], we assume that a reflection originates at the free-surface–metal boundary and at the metal–free-surface boundary, partial reflections from the neighboring boundaries must be in phase for reflections from a Λ-type structure (the boundaries are spaced by Λ/2) and in antiphase for reflections from a 0.5Λ-type structure (the boundaries are spaced by Λ/4). It is obvious that neither of these cases actually occurs. Nevertheless, the observed effects can be explained if we consider that the phases of the reflection coefficients differ considerably from 0° and 180°.

As noted in [12], an SAW reflector is the second (after the IDT) most important element of an SAW device. Through the above-described technique, new experimental results have been obtained.

This reflection-measurement technique is most appropriate in the investigation of the frequency char-

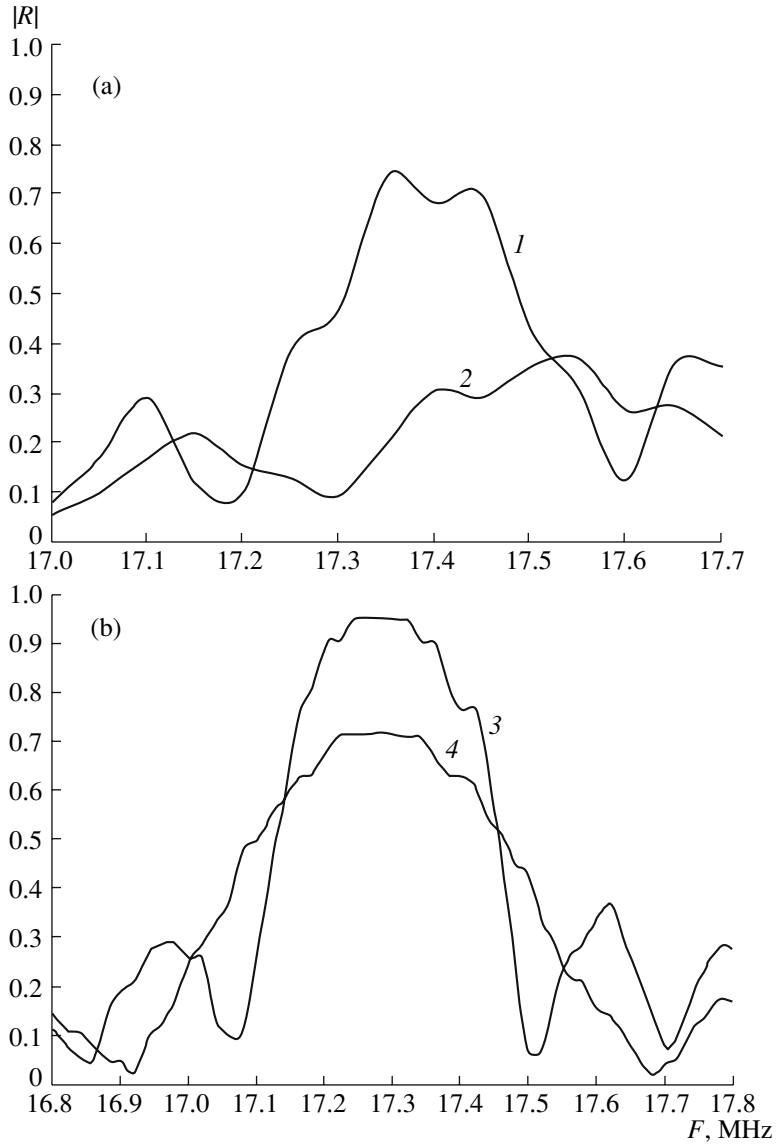

Fig. 4. Magnitude of the SAW reflection coefficient for reflection from periodic structures with periods of (a) 100 and (b) 200 μm as a function of frequency. Curves *1* and *3* correspond to $N = 40$, curve *2* corresponds to $N = 21$, and curve *4* corresponds to $N = 18$.

acteristics of reflecting objects in the range of SAW wavelengths from 500 to 30 μm. At wavelengths shorter than 30 μm, realization and tuning of the experimental facility become more difficult.

REFERENCES

1. Kh. T. Abeinayake and V. A. Komotskii, Avtometriya, No. 6, 52 (1987).
2. Kh. T. Abeinayake and V. A. Komotskii, Avtometriya, No. 3, 97 (1990).
3. I. A. Viktorov, *Rayleigh and Lamb Waves: Physical Theory and Applications* (Nauka, Moscow, 1966; Plenum, New York, 1967).
4. J. C. De Bremaecker, Geophysics **23**, 253 (1958).
5. L. Knopoff and A. P. Gangi, Geophysics **25**, 1203 (1960).
6. J. I. Burov, N. C. Thanh, and N. V. Anastasova, Appl. Phys. A: Mater. Sci. Process. **20** (2), 189 (1979).
7. A. F. Bessonov, L. N. Deryugin, and V. A. Komotskii, Opt. Spektrosk. **49**, 382 (1980).
8. V. A. Komotskii and T. D. Black, J. Appl. Phys. **52** (1), 129 (1981).
9. A. F. Bessonov, L. N. Deryugin, V. A. Komotskii, and M. V. Kotyukov, Opt. Spektrosk. **56**, 1059 (1984).
10. *Surface Wave Filters: Design, Construction, and Use*, Ed. by H. Matthews (Wiley, New York, 1977; Radio i Svyaz', Moscow, 1981) .
11. *Acoustic Surface Waves*, Ed. by A. A. Oliner (Springer-Verlag, New York, 1978; Mir, Moscow, 1981).
12. Yu. V. Gulyaev and V. P. Plesskii, Usp. Fiz. Nauk **157** (1), 85 (1981).